An Investigation on Separation Configurations in Compressor Cascades with Boundary Layer Suction (BLS)

Zhang Hualiang *Tan Chunqing* *Zhang Dongyang*
Institute of Engineering Thermophysics of Chinese Academy of Science
Beijing, 100080, China
hualiangzhang@163.com

Wang Songtao *Wang Zhongqi*
Academy of Energy Science and Engineering, Harbin Institute of Technolog
Harbin 150001, China

Keywords: Compressor, Separation Configurations, Topology, Boundary Layer Suction

Abstract

A numerical study was performed for a vane of a compressor with a high-turning angle and meridional divergence. At first, the effect of the suction position was discussed. Then, the optimal suction position was applied to the cascades with the aspect ratio of 2.53 and 0.3, respectively, to get the knowledge of the effect of the endwall boundary layer removal on the secondary flow along the blade height. At last, using the critical principles of the three-dimensional separation, the topological structures of the flow patterns of the body surfaces and the separation configurations were discussed in detail. The results show that the largest reduction of the total loss can be achieved when the suction slot is near the suction side. The topological structure as well as the separation configuration varies due to boundary layer removal, which restrains the flow separation at the corner and delays or depresses the separation on the suction surface. Compared with the original cascade, the cascade with the endwall boundary layer removal has a higher blade loading along the most span. Furthermore the flow loss decreases and distributes uniformly along the span.

Nomenclature

N	=	nodal point
S	=	saddle point
P	=	static pressure
P^*	=	total pressure
T^*	=	total temperature
k	=	specific heat ratio of air
$\bar{z}$	=	axial chord length
$\bar{\xi}$	=	pitch-averaged energy loss coefficient
$\bar{R}$	=	relative height of the blade
$\bar{C}_p$	=	static pressure ratio
τ	=	aspect ratio of the cascade
PS	=	pressure side of the cascade
SS	=	suction side of the cascade
MP	=	mid-passage of the cascade
STR	=	original cascade
BLS	=	cascade with boundary layer suction

subscripts

1	=	inlet of the cascade
2	=	outlet of the cascade

Introduction

With the development of the modern aviation, a further improvement of the aero-engines performance is required. The compressors with a higher pressure ratio, a higher loading as well as enhanced stability are desired.[1)] It is well-known that an increase in flow turning angle is available to a higher blade loading. However, a high-turning angle will increase the thickness of the boundary layer and induce flow separation. Sometimes, the flow separation is three-dimensional and cannot be avoided only through the geometrical modifications of the blade profiles. By far, many attempts have been made to gain high loading and at the same time to reduce loss resulted from the flow separation such as Wennerstrom,[2)] who clarified that the boundary layer control was available to increase the loading besides applying low aspect ratio cascades and splitters. Nowadays the application of boundary layer suction has become an interesting design method in high-turning and highly-loaded compressors.

As early as 1971, Loughery[3)] studied the effect of boundary layer suction on the compressors and concluded that suction can improve the aerodynamic performance of the compressor cascades. In 1997, Kerrebrock[4)] discussed the concept of aspirated compressors, addressing that boundary layer suction just at the shock impingement location on the suction surface of transonic compressor blades could increase flow turning, flow capacity and efficiency. Generally, removal of low energy fluid at critical locations could produce approximately twice the work realized without boundary layer suction. Then MIT designed three fan stages with the pressure ratio of 1.5 at a tip speed of 213 m/s, the pressure ratio of 2.0 at a tip speed of 305 m/s and the pressure ratio of 3.0 at a tip speed of 457 m/s. The measured adiabatic efficiencies were 94%, 92% and 87%, respectively.[5)] In addition, Reijnen[6)] tested a transonic compressor stage with boundary layer suction and demonstrated that the thinner boundary layer by suction could increase the turning angle as well as the pressure ratio.

Furthermore, a delay of stall was observed in his experiments. However the effect of boundary layer suction on the separation configuration in the high-turning cascades has not been investigated in detail by far. On the other hand, the proportion of the endwall loss to the total loss enlarges due to the development of the compressors with highly-loading as well as low aspect ratio. So, a special investigation on endwall boundary layer removal is essential.

The application of topological analysis to fluid mechanics was started in the investigation on the behavior of limiting streamlines first adopted by Sears.[7] Legendre[8] et al. went further into the postulate of continuous vector fields constructed by the limiting streamlines, and studied the natures of singular points of finite number in the vector fields. So far, topological analysis has been widely and successfully used in the studies of external flows, such as those by Maskell,[9] Lighthill,[10] Tobak,[11] and Perry,[12] and in the studies of internal flows, such as those by Delery,13) Gbadebo,14) and so on.

The focus of this paper is to study numerically the application of endwall boundary layer suction to a vane of a compressor, and to discuss the mechanism of the loss reduction due to the boundary layer removal through analyzing the variation of the separation configurations using the topological principles.

Numerical procedure

The numerical simulations were carried out for a compressor vane with meridional divergence as well as a turning angle of about 50°. The suction was applied to the cascades with $\tau = 2.53$ and $\tau = 0.3$, respectively, to get the knowledge of the effect of endwall boundary layer suction on the secondary flow along the whole blade height.

The Mach number of inlet flow was 0.75, and the inlet flow angle was 43°. The calculations were performed using the CFD package Fine/Turbo of NUMECA under the same boundary conditions, such as P_1^*=525000 Pa, T_1^*=500 K and P_2=460000 Pa, on structured multi-block grids. The mesh consisted of 49 ×65×113, in the tangential, radial, and streamwise directions for the cascade with τ=2.53, and 49×41× 113 for the cascade with τ=0.3. And the value of y^+ was less than 3. An explicit time marching, implicit residual smoothing four-step Runge-Kutta procedure and the turbulence model of k-epsilon (Low Re Yang-Shih model) were used in steady state mode. Local time stepping and multi-grid capability were applied to accelerate convergence.

Result and Discussion

Effect of the suction position

At first, the effect of the suction position on the total loss was discussed in this paper. Figure 1 shows the different positions of the suction slots on the endwall. The first suction slot was opened near suction side, the second suction slot was opened near the mid-passage, and the last suction slot was opened near pressure side. The suction slots had the same direction as that of the first axial mesh adjacent to the endwall and had a width of two meshes. The flow rate from every slot was 1% of the inlet flow according to the discussions of the documents.[15] The flow details inside the slot were not given in this paper although different static pressures inside the slot were set to get the desired suction flow rates. Figure 2 shows the radial distributions of the pitch-averaged energy loss coefficient at 40% of chord length downstream the blade trailing. The pitch-averaged energy loss coefficient is defined by:

$$\overline{\xi} = \frac{\left(P_2 / P_2^*\right)^{(k-1)/k} - \left(P_2 / P_1^*\right)^{(k-1)/k}}{1 - \left(P_2 / P_1^*\right)^{(k-1)/k}} \qquad (1)$$

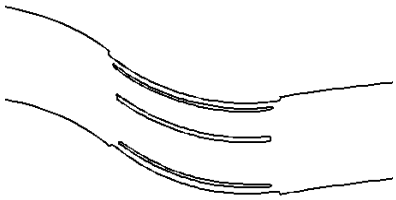

(a) Hub

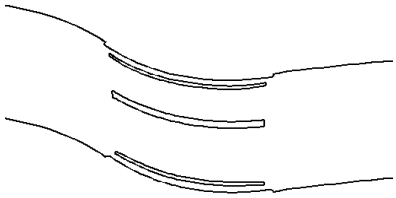

(b) Shroud

Fig.1 Suction slots positions on endwalls

It can be seen that the largest reduction of the total loss is obtained when the suction slot is near suction surface. When the suction slot is opened near the mid-passage or near pressure surface, however, boundary layer removal does not improve the flow performance, and increases the loss near the endwall contrarily. The high turn of the cascade may be the cause, which induces a serious flow separation at the corner. When the suction slot is near suction side, suction can remove the low energy fluid just at the corner, so the corner separation is depressed. When the suction slot is near the mid-passage, the low energy fluid collected at the corner moves to the mid-passage, which induces the starting point of the corner separation to move upstream and the range of the flow separation to enlarge in pitch-wise. When the suction slot is near pressure surface, although the low energy fluid also has the trend to the mid-passage, this motion is feasible because of the increase in the distance between the slot and suction side. Especially in the case of τ=0.3, because the flow passage is narrower, all kinds of flow separations in the cascade commix seriously and the flow is very complex. The application of boundary layer suction on the endwall near suction side is discussed in the following sections.

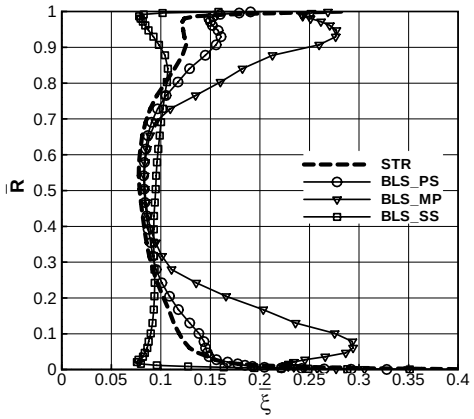

(a) τ=2.53

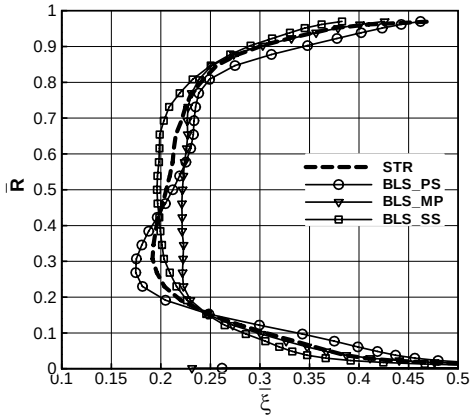

(b) τ=0.3

Fig.2 Radial distribution of pitch-averaged loss coefficient

Topology of the surface streamlines pattern

The pattern of the limiting streamlines is always composed of several critical points for any given flow. Generally the number, type, and distribution of the critical points are called the topological structure of the surface pattern. Through studying the local property of the critical points and their global character on the body surface, we can discover much information on the flow. For example, a saddle point means local inverse flow and to form a closed separation, a spiral point often is the starting point of a so-called concentrated shed vortex, which makes the flow more complex. So, more critical points mean more flow losses. In addition, there are several topological principles about the flow patterns: (1) If the separation line starts from a critical point, this critical point must be a saddle point; if the separation line ends at a critical point, this critical point must be a nodal point.[16] (2) If many critical points are distributed on the separation line, two saddle points or two nodal points cannot directly connect each other along the separation line, i.e. the saddle point and the nodal point must appear alternatively.[16]

Figure 3 and Figure 5 show the calculated results of the limiting streamlines over the cascade surface. Figure 4 and Figure 6 show the topology sketches of the surface patterns of the original cascades and the cascades with boundary layer suction by using the topological principles above. Because the flow is attached on the pressure surface, and there is no obvious radial secondary flow in all instances, the flow patterns on the pressure surface are not shown in this paper.

(1) τ=2.53

It can be seen from Fig. 3(a) and Fig. 4(a) that the uniform coming flow, approaching the blade leading edge, splits into two branches at a saddle point in front of the leading edge, from which the fluid rolls up and forms the suction side leg and the pressure side leg of the horseshoe vortex. The passage vortex, coming from the boundary layer on the endwall, is a classical open separation, which originates from a regular point so that the original position of the three-dimensional separation is difficult to be determined. The flow pattern on suction surface is complex. There are two separation lines, labeled as S_6N_3 and S_7N_4, which end at separation spiral points, N_3 and N_4, respectively. Along the separation lines the boundary layer rolls up, circuits around the spiral points and forms two so-called concentrated shed vortex. These spiral vortices take vast of low energy fluid downstream with an obvious vortex core and commix with the so-called trailing shed vortex so that the loss increases remarkably. In addition, there are two radial separation lines, labeled S_8N_3 and S_8N_4, near the trailing edge of the blade, from which the trailing shed vertex evolves. These separation lines cannot be seen commonly in the calculations as well as in the experiments, but it ought to exist through the topological analysis. It is noticeable that the flow separation on the upper part of the blade is more serious in comparison with that on the lower part because of a lower solidity as well as the effect of the meridional divergence. The upper separation begins at a saddle point, S_5, and ranges from 15% of chord length to the exit in the axial direction, from 70% of blade length to the tip in the radial direction and up to 20% pitch in the pitch-wise direction. It is a closed separation with a visible bubble. The separation on the lower part of the blade only occurs on suction surface. The number of saddle points is 8, and the number of nodal points is 6 in the topological sketch.

The limiting streamlines on the cascade surface with endwall boundary layer removal, shown in Fig. 3(b) and Fig. 4(b), vary obviously. Boundary layer removal near suction side holds back the collection of the low energy fluid at the corner, especially near the casing, the effect of the meridional divergence is also reduced so much that the separation bubble does not occur. Furthermore the flow pattern of the cascade with suction is simpler than that of the original cascade. The range of flow separation reduces and the closed separation at the corner disappears. Because the main flow separation is the trailing shed vortex, which is similar to the free vortex surface separation, and its mixing loss is less than the bubble separation, so the total loss reduces markedly. However, it is noticeable that the local loss near the midspan increases because the inverse flow increases there as the variation of the separation configuration. Topology sketch shows that

the number of saddle points is 5, the number of nodal points reduces to 1, i.e. the total number of the critical points decreases.

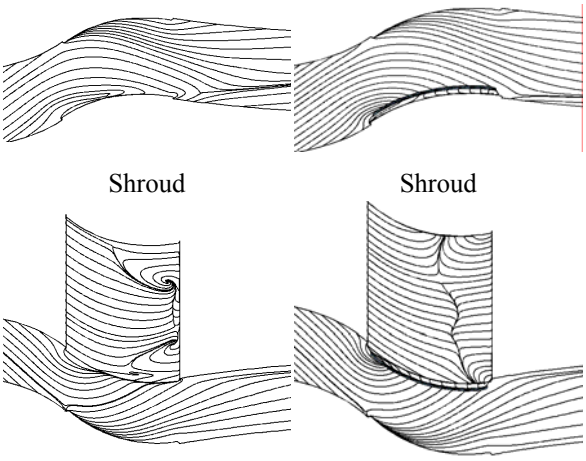

Fig.3 Calculated limiting streamlines with $\tau=2.53$

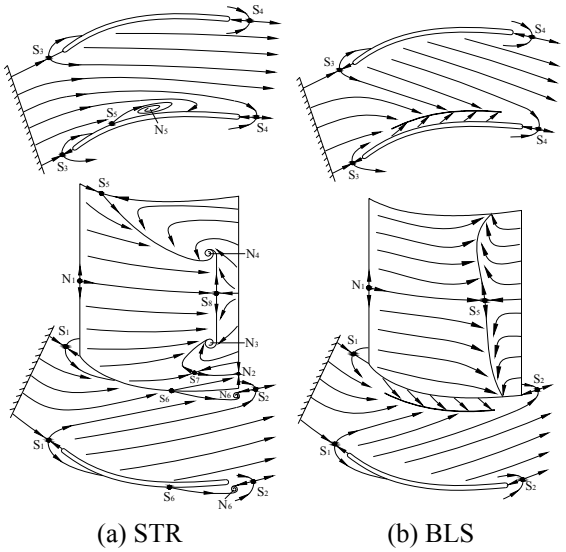

Fig.4 Topology sketch of the surface flow pattern with $\tau=2.53$

(2) $\tau=0.3$

Because the flow passage of the cascade with $\tau=0.3$ is narrower than that of the cascade with $\tau=2.53$, the effect of the meridional divergence is more remarkable. Figure 5(a) and Figure 6(a) show that the inverse flow due to the serious separation occupies 60% of the whole suction surface. This separation, converging at a separation spiral point N_2, also rolls up from the boundary layer on the suction surface and develops downstream with a obvious vortex core. So it can be called as concentrated shed vortex. The flow of the upper part of the blade has the character of the bubble separation (closed separation) and the flow of the lower part of the blade mixes with the upper bubble at last. There is no clear borderline between the two parts. According to this property of the flow forbidden zone, we can regard the separation on the suction surface as closed separation on the whole. Topology sketch shows that the total number of nodal points and saddle points is 5 and 7, respectively. For the cascade with boundary layer suction, the suction also restrains the separation at the corner as shown in Fig. 5(b) and Fig. 6(b). The surface flow pattern changes obviously. There is a typical structure of one saddle point linked with double spiral points. The separation, starting from saddle point, S_7, splits into two separation lines labeled S_7N_2 and S_7N_3 respectively and ends at two spiral points labeled N_2 and N_3, from which two concentrated shed vortexes form. Although the separation configuration still belongs to closed separation, the separation range reduces markedly in comparison with the original cascade so that the total loss reduces. Similarly, the local loss near the mid-span increases because the inverse flow increases due to the variation of the separation configuration. Topology sketch shows the number of nodal points is 3, the number of saddle point is 7. The total number of the critical points reduces, and the topological structure of the flow pattern becomes simple, so the flow is more organizational.

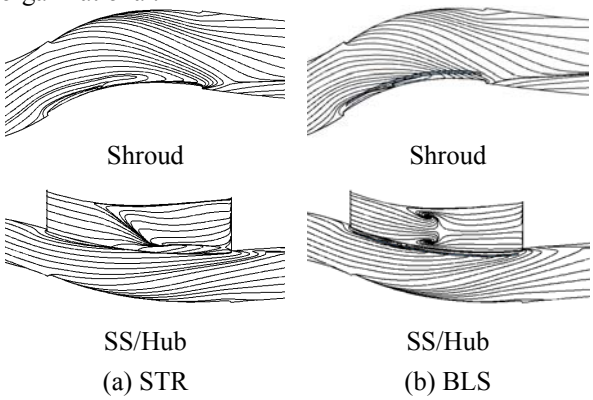

Fig.5 Calculated limiting streamlines with $\tau=0.3$

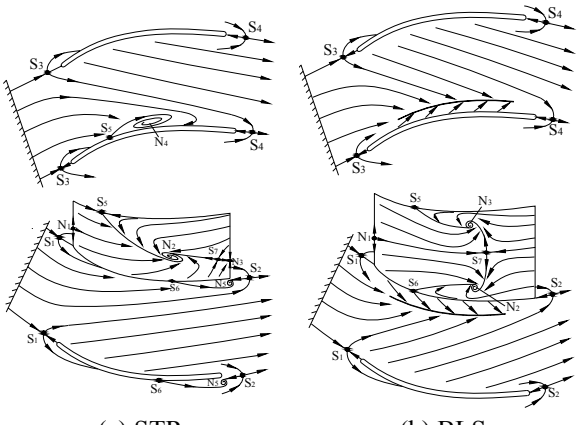

Fig.6 Topology sketch of the surface flow pattern with $\tau=0.3$

It can be concluded from the discussions above that boundary layer suction reduces the critical points and alters the topological structures of the surface flow pattern so that the separation configurations become simple, and the flow performance is improved.

Pitch-average energy loss and load distribution

In general, the study of the limiting streamline patterns enables us to obtain a certain amount of information about the whole three-dimensional flow structure. However, surface flow pattern alone can not provide a complete interpretation of the whole field. Studying three-dimensional flow separation also requires the discussion of other flow parameters. Figure 7 shows the radial distributions of the pitch-averaged energy loss coefficient at 40% of chord length downstream of the blade trailing. It can be seen that the loss decreases distinctly and distributes uniformly along the most span when the suction flow rate is only 1% on every endwall. The loss decreases markedly from hub to 25% of blade length and from 75% of blade length to the tip due to boundary layer removal when $\tau = 2.53$. The loss falls from hub to 15% of blade length and from 45% of blade length to the tip due to the application of suction when $\tau = 0.3$. The loss reduction is the result of the variations of the surface flow pattern as well as the separation configurations. However the loss near the midspan increases partly, which is consistent with the local inverse flow strengthening on the surface flow pattern. In other word, the variations of the separation configurations re-arrange the distributions of the loss. The result also indicates that the flow separation on suction surface can not be entirely diminished only through endwall boundary layer suction.

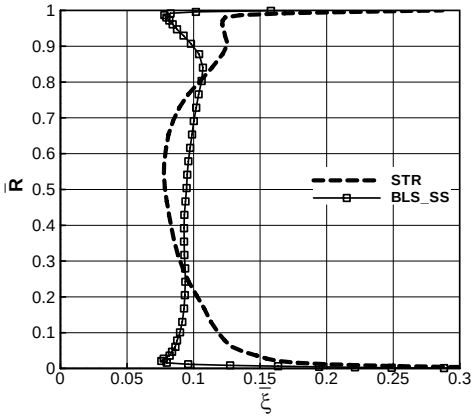

(a) $\tau = 2.53$

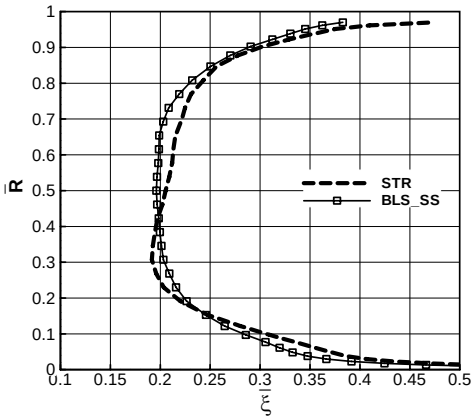

(b) $\tau = 0.3$

Fig.7 Radial distribution of pitch-averaged loss coefficient

The axial distributions of the static pressure coefficient on the blade surfaces are shown in Fig. 8 and Fig. 9. The static pressure coefficient in this paper is defined as Local/Exit. The blade loading of the cascade with boundary layer removal increases in comparison with that of the original cascade. Furthermore this tendency is more obvious near endwall. As the aspect ratio is 0.3, the loading increases along the whole blade height.

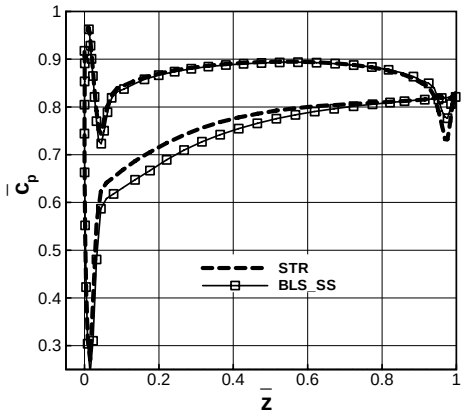

(a) 5% $\bar{R}$

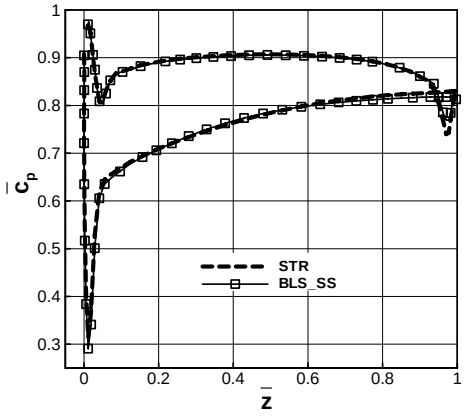

(b) 50% $\bar{R}$

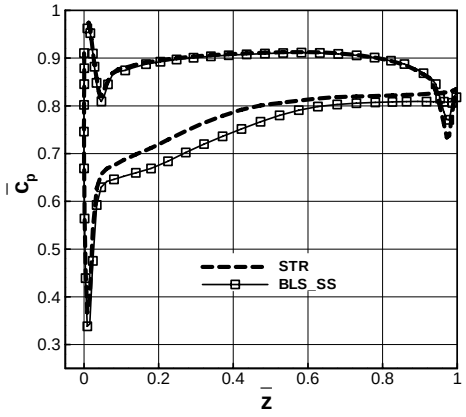

(c) 95% $\bar{R}$

Fig.8 Axial Static pressure coefficient at different blade height with $\tau = 2.53$

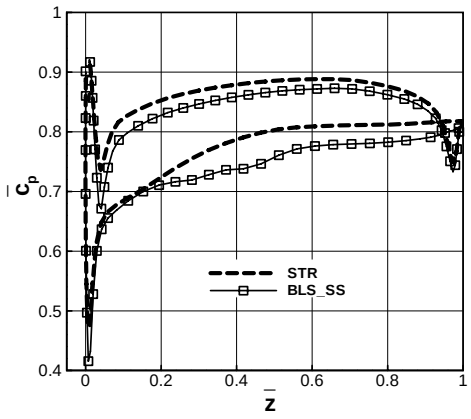

(a) 5% $\bar{R}$

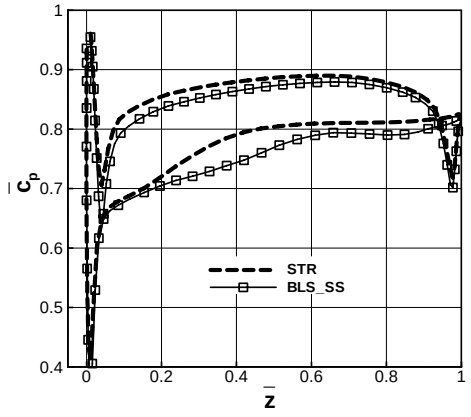

(b) 50% $\bar{R}$

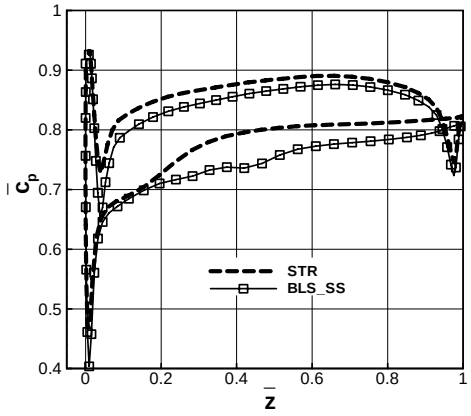

(c) 95% $\bar{R}$

Fig.9 Axial Static pressure coefficient at different blade height with $\tau = 0.3$

Conclusion

In this article, a study was performed for a vane of a compressor with a high-turning angle. Some conclusions are gained as follows:

(1).Endwall boundary layer suction reduces the total number of the critical points so as to change the topological structure of the surface flow pattern. The variation of the surface flow pattern reveals the variation of the separation configuration. As a result, the flow becomes more organizational.

(2).The optimal suction position on the endwall is near suction side. The closed separation at the corner is avoided and the separation on suction surface is delayed or diminished due to the removal of boundary layer on the endwall, which increases the loading along the most span. Furthermore the loss distributes uniformly along the span.

(3).The variation of the separation configuration changes the distribution of the loss from which we can see an improvement of the total performance due to the endwall suction. However, the loss may be increase in a local region such as the midspan, which also proves that only application of endwall suction cannot eliminate entirely the separation on suction surface.

This paper only discussed boundary layer suction on the endwall, the application of boundary layer suction to the blade itself was not carried out. How to achieve the optimal performance through combining the endwall suction with the blade suction needs deeply investigations.

Acknowledgment

The authors would like to acknowledge the support of the National Natural Science Foundation of China, grant no. 10577019

References

1) Bogod, A. B.: Direct and Inverted Calcutation of 2D Axisymmetric and 3D Flows in Axial Compressor Blade Rows, TsAGI, Moskow, Russia, 1992.
2) Wennerstrom, A. J.: Highly Loaded Axial Flow Compressor: History and Current Development, *Journal of Turbomachinery*, 1990, Vol. 112, pp. 567-578.
3) Loughery, R., Horn, R. A.: Single Stage Experimental Evaluation of Boundary Layer Blowing and Bleed Techniques for High Lift Stator Blades, NASA, 1971, CR-54573.
4) Kerrebrock, J. L., Reijnan, D. P., Ziminsky, W. S., and Smilg, L. M.: Aspirated Compressors, ASME Paper, 1997, 97-GT-525.
5) Kerrebrock, J. L., Drela, M., Merchant, A. A.: A Family of Designs for Aspirated compressors, ASME Paper, 1998, 98-GT-196.
6) Reijnen, D. P.: Experimental Study of Boundary Layer Suction in a Transonic Compressor, PhD Thesis, MIT, Cambridge, MA, January, 1997.
7) Sears, W. R., "The Boundary Layer of Yawed Cyliners", *J. of Aerospace Sciences*, 1948, Vol. 15, No. 1, pp. 49-52.
8) Legendre, R.: Linges de Conrant d'un Ecoulement Coutinu, La Recherche Aerospatiale, No. 105, 1965, pp. 3-9
9) Maskell, E. C.: Flow Separation in Three Dimensions, RAE Farnborough Report, 1955, No. 2565.

10) Lighthill, M.J.: *Attachment and Separation in Three-Dimensional Flows, Laminar Boundary Layers, ed. L. Rosenhead*, Oxford Univ. Press, 1963, pp.72-82.
11) Tobak, M., and Peake, D. J.: Topology of Three-Dimensional Separation Flows, *Annual Review of Fluid Mechanics*, 1982, Vol. 14, pp. 61-85.
12) Perry, A. E., and Chong, M. S.: A Description of Eddying Motions and Flow Patterns Using Critical Point Concepts, *Annual Review of Fluid Mechanics*, 1987, Vol. 19, pp. 125-155.
13) Delery, J., and Meauze, G.: A Detailed Experimental Analysis of the Flow in a Highly Loaded Fixed Compressor cascade: the Iso-Cascade Co-operative Programme on Code Validation, *Aerospace Science and Technology*, 2003, Vol.7, No.1, pp. 1-9.
14) Gbadebo, S. A., and Cumpsty, N. A.: Three-Dimensional Separations in Axial Compressors, ASME paper, 2004, GT2004-53617.
15) Song,Y. P., Chen, F., Yang, J., Wang, Z. Q.: A Numerical Investigation of Boundary Layer Suction in Compound Lean Compressor Cascades, ASME Paper, 2005, GT2005-68441.
16) Zhang, H. X.: Analytical Study of Three-Dimensional Separated Flows, *Progress in Natural Science*, 1995, Vol.5, No. 2, pp. 238-240.